

아세트산 에틸 제거를 위한 공침법 기반의 Cu 및 Mn 이종금속 촉매의 제조

김민재 · 윤조희 · 정재민^{*,†} · 최봉길[†]

강원대학교 화학공학과, *한국지질자원연구원
(2022년 7월 11일 접수, 2022년 8월 7일 수정, 2022년 8월 24일 채택)

Preparation of Cu and Mn Bimetallic Catalyst Based on Co-Precipitation Method for Removal of Ethyl Acetate

Min Jae Kim, Jo Hee Yoon, Jae-Min Jeong^{*,†} and Bong Gill Choi[†]

Department of Chemical Engineering, Kangwon National University, Samcheok 25913, Republic of Korea

*Mineral Resources Research Division, Korea Institute of Geoscience and Mineral Resources, Daejeon 34132, Republic of Korea

(Received July 11, 2022; Revised August 7, 2022; Accepted August 24, 2022)

초 록

최근 촉매 소각 공정은 휘발성 유기 화합물을 저온(< 450 °C)에서 고효율(> 95%)로 산화 및 분해하기 위해 상당한 주목을 받고 있다. 많은 귀금속 촉매 물질이 잘 연구되어 사용되고 있으나 단가가 비싸고 위험하다. 본 연구에서는 Cu와 Mn 전구체의 공침법을 활용하여 간단하고 손쉬운 합성 방법을 개발함으로써 고효율 및 저비용의 Cu-Mn 바이메탈 촉매를 제조하였다. 촉매 합성은 Cu와 Mn의 조성비를 조절하여 최적화하였다. 최적화된 촉매는 메조포러스 구조로 230.8 m²/g의 넓은 표면적을 나타냈다. 촉매 성능을 입증하기 위해 에틸 아세테이트의 산화 반응에 대해 Cu-Mn 촉매를 테스트했으며, 250 °C의 저온에서 100%의 높은 전환 효율을 나타내었다.

Abstract

The catalytic thermal oxidizer process has recently attracted considerable attention for the oxidation and decomposition of volatile organic compounds at low temperatures (< 450 °C) with high efficiency (> 95%). Although many noble metal catalytic materials are well established, they are expensive and hazardous. Herein, highly active and low-cost Cu-Mn bimetallic catalysts were prepared using a simple and facile synthesis method involving the co-precipitation of Cu and Mn precursors. The synthesis of the catalyst was optimized by controlling the composition ratio of Cu and Mn. The optimized catalyst exhibited a large surface area of 230.8 m²/g with a mesoporous structure. To demonstrate the catalytic performance, the Cu-Mn catalyst was tested for the oxidation reaction of ethyl acetate, showing a high conversion efficiency of 100% at a low temperature of 250 °C.

Keywords: VOCs, Copper, Manganese, Catalyst, Catalytic thermal oxidizer

1. Introduction

Volatile organic compounds (VOCs) are produced in industrial manufacturing (e.g., inks, paints, films, and cosmetics) and have a high vapor pressure at room temperature and low boiling point [1-4]. Common VOCs include ethylene glycol, formaldehyde, methylene chloride, toluene, xylene, benzene, and ethyl acetate (EA). Some VOCs have harm-

ful effects on human health and the environment [1,2]. Regenerative thermal oxidizer (RTO) technology has been utilized as a representative process for removing VOCs [5,6]. This process oxidizes and decomposes VOCs at 800 °C or higher, thus providing high removal efficiency of VOCs (> 98%). However, the high temperature of RTO requires high energy consumption, resulting in high processing costs. As an alternative technology, a catalytic thermal oxidizer (CTO) process has also been suggested for removing VOCs [7,8]. High-performance catalysts enable oxidizing VOCs at a relatively low temperature of 300-450 °C with a high removal efficiency of > 95%.

Numerous catalytic materials have been exfoliated to remove VOCs in the CTO process, including noble metal (e.g., Pt, Pd, Ru, and Au) and transition metal (e.g., Cu, Mn, Co, Ti, Ni, V, and Fe) oxides [9,10]. Noble metals are expensive and hazardous; in contrast, transition metal oxides are relatively low-cost, environmentally friendly,

† Corresponding Author: Jae-Min Jeong: Department of Chemical Engineering, Kangwon National University, Samcheok 25913, Republic of Korea; Bong Gill Choi: Mineral Resources Research Division, Korea Institute of Geoscience and Mineral Resources, Daejeon 34132, Republic of Korea
Tel: Jae-Min Jeong: +82-42-868-3503 ; Bong Gill Choi: +82-33-570-6545
e-mail: Jae-Min Jeong: jmjeong@kigam.re.kr; Bong Gill Choi: bgchoi@kangwon.ac.kr

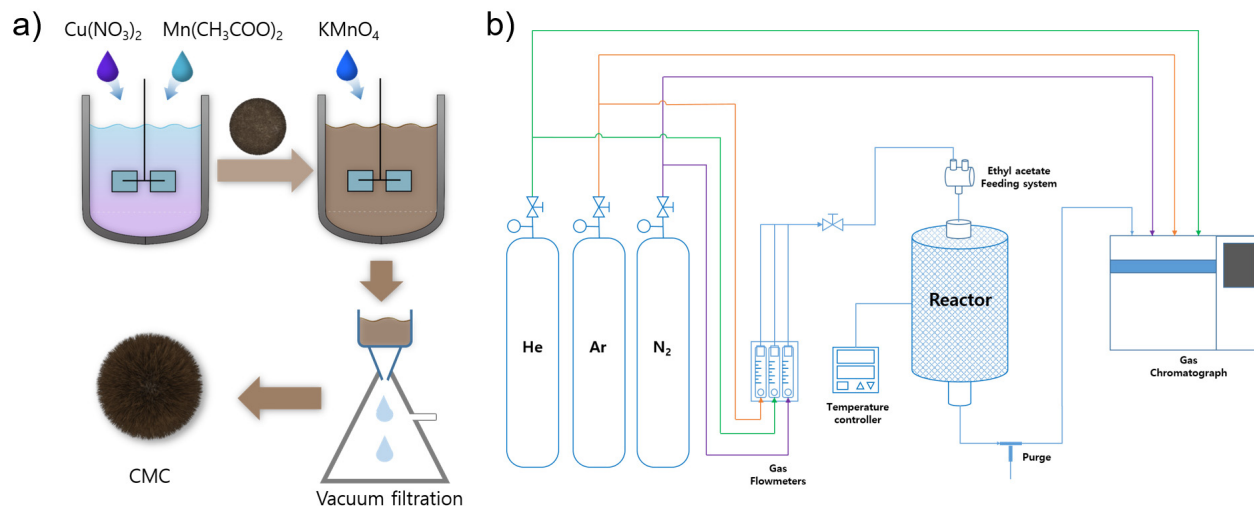


Figure 1. Schematic of (a) preparation of CMC catalyst using co-precipitation of Cu and Mn precursors and (b) catalytic test system for the oxidation reaction of EA.

and highly active for the combustion of VOCs[1-3]. Among the transition metal oxides, Cu-Mn bimetallic catalysts exhibit high catalytic performance with a removal efficiency of $> 95\%$ at a low operating temperature of $250\text{ }^\circ\text{C}$ [4]. Numerous Cu^{2+} and Mn^{4+} cations play a critical role in the catalyzed oxidation of VOCs[11]. The composition ratio of Cu to Mn leads to different phases, morphologies, and structures, influencing the catalytic performance[12]. Therefore, an optimized synthesis method is required to control the formation of the Cu-Mn catalyst (CMC).

In this study, we prepared a CMC using a simple and facile co-precipitation method. During the synthesis of the heterogeneous catalyst, the Mn: Cu weight ratio of 4:1 was maintained by controlling the concentration of the Cu precursors (2.5~80 mM). CMC with 5 mM Cu concentration exhibited a large surface area of $230.8\text{ m}^2/\text{g}$ with a mesopore structure. The resultant CMC was used as a heterogeneous catalyst for the selective oxidation of EA molecules to acetic acid and ethane. The CMC exhibited an excellent conversion efficiency of 100% after 1 h at $220\text{ }^\circ\text{C}$.

2. Experimental

2.1. Chemicals

The chemicals required for the study, $\text{Mn}(\text{CH}_3\text{COO})_2 \cdot \text{H}_2\text{O}$, KMnO_4 , and cupric $\text{Cu}(\text{NO}_3)_2 \cdot \text{H}_2\text{O}$ were purchased from Sigma-Aldrich (USA). Acetone and ethanol were procured from Junsei Chemical Co. Ltd. (Japan). All the chemical reagents were used without further purification.

2.2. Synthesis of CMC

CMC was synthesized by co-precipitation method[Figure 1(a)] using $\text{Mn}(\text{CH}_3\text{COO})_2 \cdot \text{H}_2\text{O}$, KMnO_4 , and $\text{Cu}(\text{NO}_3)_2 \cdot \text{H}_2\text{O}$ in an Mn: Cu weight ratio of 4:1. $\text{Mn}(\text{CH}_3\text{COO})_2 \cdot \text{H}_2\text{O}$ and KMnO_4 were mixed in deionized water, and $\text{Cu}(\text{NO}_3)_2 \cdot \text{H}_2\text{O}$ was added to the resultant

mixture. Following the co-precipitation process, the products were washed several times with acetone, ethanol, and deionized water. CMC powder samples were obtained after aging at $80\text{ }^\circ\text{C}$ for 12 h. CMC synthesis was systematically investigated by controlling the concentration of the copper precursor (2.5~80 mM, fixed at a weight ratio of Mn:Cu = 4:1), reaction time (1~30 min), and reaction temperature ($25\text{--}80\text{ }^\circ\text{C}$). Note that previous reports described the effects of composition ratio of Mn and Cu on the catalytic performance[13]. Also, a commercially available hopcalite Mn/Cu catalyst includes 4:1 composition ratio of Mn and Cu.

2.3. Material characterization

Scanning electron microscopy (SEM) images were obtained using a field-emission scanning electron microscope (JSM-6701F, JEOL, Ltd.). Optical microscopy images were obtained using an optical microscope (BX53MTRF-S; OLYMPUS). N_2 adsorption/desorption was determined by Brunauer-Emmett-Teller (BET) measurements using an ASAP-2010 surface area analyzer. X-ray diffraction (XRD) data were obtained using a Rigaku D/MAX-2500 (40 kW) diffractometer with a θ/θ goniometer equipped with a Cu $K\alpha$ radiation generator.

2.4. Catalyst characterization

The catalytic activity of CMC for the catalytic decomposition of EA was investigated using a gas-phase fixed-bed reactor in the temperature range of $150\text{--}250\text{ }^\circ\text{C}$ [Figure 1(b)]. The flow rates of each gas path were calculated based on the saturated vapor pressure of the EA and were controlled by mass flow meters. The CMC samples were tested in parallel, using the same reactant feed stream. The concentration of EA in the air was 1000×10^{-6} and the gas hourly space velocity was 12500 h^{-1} . The conversion efficiency of EA was analyzed using a gas chromatograph (Tremetrics 9001) equipped with an HP-5 column and FID detector. The conversion efficiency of EA was calculated as follows:

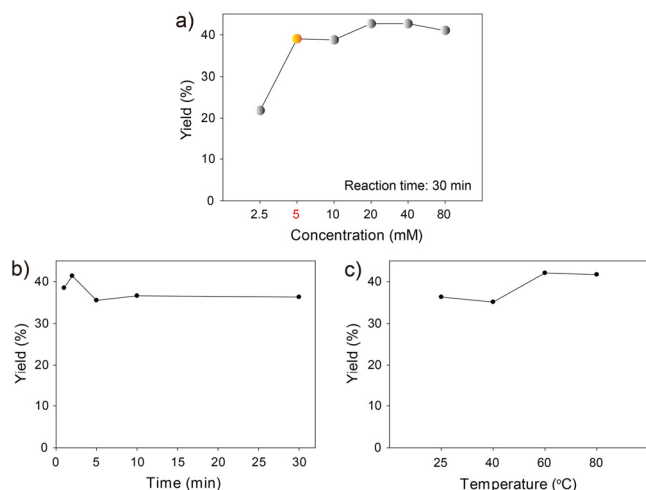


Figure 2. CMC yields obtained from (a) different Cu concentrations, (b) different reaction times, and different reaction temperatures.

$$X = \frac{C_{in} - C_{out}}{C_{in}} \times 100\% \quad (1)$$

where C_{in} and C_{out} represent the inlet and outlet concentrations of EA, respectively.

3. Results and discussion

Figure 1(a) illustrates the preparation method for CMC by the co-precipitation of $Mn(CH_3COO)_2 \cdot H_2O$, $KMnO_4$, and $Cu(NO_3)_2 \cdot H_2O$ in an Mn: Cu weight ratio of 4:1. The synthesis method involved a two-step process for the efficient synthesis of CMC. $Mn(CH_3COO)_2 \cdot H_2O$ and $KMnO_4$ were mixed in the first step, and $Cu(NO_3)_2 \cdot H_2O$ was added in the second step. CMC was obtained after filtering and aging at 80 °C for 12 h. The co-precipitation procedure was based on the redox process and electron transfer between Cu^+ , Mn^{2+} , and Mn^{7+} according to the following reaction: $Cu^+ + Mn^{2+} + Mn^{7+} \rightarrow Cu^{2+} + 2Mn^{4+}$ [14]. To investigate the yield of CMC, the precursor concentration, reaction time, and reaction temperature were manipulated during the co-precipitation process. The concentration of the copper precursor varied in the range of 0.0025–0.08 M with a fixed Mn: Cu weight ratio of 4:1. The synthesis was also performed at different times (1–30 min) and temperatures (25–80 °C).

Figure 2(a) shows the yield of CMC obtained from different concentrations of the Cu precursor at a reaction temperature of 25 °C and a reaction time of 30 min. A low concentration of 2.5 mM resulted in a low yield of 21.5%. When the concentration was increased to 5 mM, the yield performance increased significantly to 38%. Further, increasing the concentration from 0.005 M to 8 mM exhibited a similar yield of 41%. A concentration of 5 mM for the Cu precursor was optimized for a high yield of CMC. Therefore, the synthesis of CMC with a 5 mM Cu precursor was further investigated at different times [Figure 2(b)] and temperatures [Figure 2(c)]. Although reaction times of 1 and 3 min showed higher yields compared to other reaction times, the

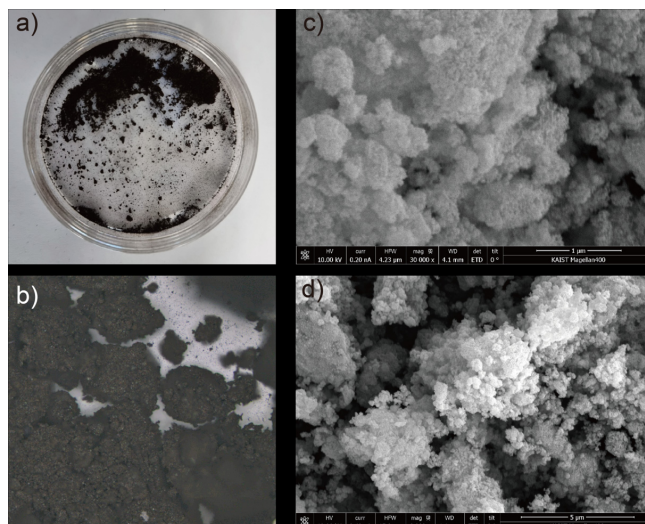


Figure 3. (a) Photograph and (b) optical images of 5-CMC. SEM images of (c) 5-CMC and (d) 8-CMC.

as-obtained CMC in a short reaction time had a poor crystalline structure and low specific surface area ($< 30 \text{ m}^2/\text{g}$) of copper and manganese oxide, which is not suitable for application in catalytic thermal oxidation reactions[15,16]. Higher reaction times of 10 and 30 min resulted in similar yields for the synthesis of CMCs. Increasing the reaction temperature from 25 to 80 °C increased the yield performance from 38% to 41.5%. The experimental parameters of time and temperature in this study exhibited a subtle change in yield performance. The crystalline structure and textural properties of catalysts can be influenced by precursor concentrations in synthetic conditions. Based on these results, we selected two CMC samples obtained using different Cu precursor concentrations of 5 mM and 80 mM at 25 °C for 30 min. The CMC samples were denoted as 5-CMC and 8-CMC for Cu precursor concentrations of 5 mM and 80 mM, respectively.

Photographs and optical images of 5-CMC showed a dark brown fine powder sample [Figures 3 (a), and (b)]. Examination of the SEM images revealed that the 5-CMC and 8-CMC samples had aggregated nanoparticles [Figures 3 (c), and (d)]. The randomly aggregated CMC nanoparticles resulted in numerous empty voids and pore structures, which is favorable for enhancing catalytic performance. The crystalline structure of CMC was investigated using XRD measurements. Figure 4(a) shows the XRD patterns of the as-synthesized CMC samples. The diffraction peaks at 2θ values of 38.4°, 48.7°, and 67.7°, which were ascribed to the (111), (202), and (113) planes, respectively, were indexed to CuO (JCPDS 01-089-2529)[3,4]. The other main diffraction peak at 18.7° corresponds to the (111) plane of manganese oxide (MnO_2 , JCPDS 01-083-6090)[3,4]. These diffraction peaks indicated the coexistence of copper and manganese oxides in the 5-CMC and 8-CMC samples. Nitrogen adsorption and desorption measurements were performed to investigate the BET surface areas of the CMC samples. Figure 4(b) shows the hysteresis loop of the type IV isotherm, indicating the mesoporous structure of CMC. The mesopores of CMC are mainly attributed to the aggregated voids of the self-as-

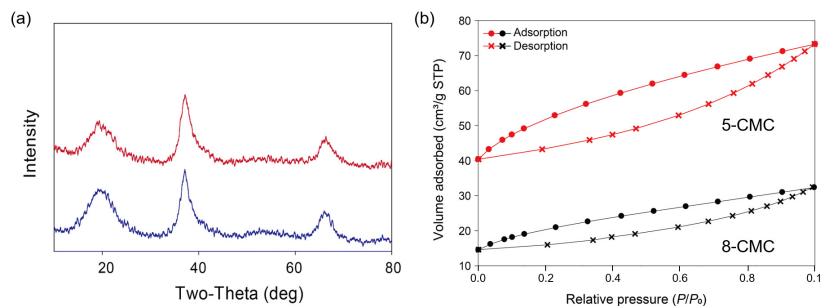


Figure 4. (a) XRD patterns and (b) nitrogen adsorption and desorption profiles of 5-CMC and 8-CMC.

sembled nanoparticles. A large surface area of $230.8 \text{ m}^2/\text{g}$ for 5-CMC was obtained using the BET equation. This surface area is two-fold higher than $103.3 \text{ m}^2/\text{g}$ of 8-CMC.

The catalytic performance of the CMC catalysts was demonstrated by the oxidation of EA in a fixed-bed reactor at atmospheric pressure. Figure 1(b) shows a schematic of the catalyst test system of a gas-phase fixed-bed reactor connected to a gas flowmeter, temperature controller, and gas chromatograph. The use of the CMC catalyst facilitated the oxidation of EA to acetate and ethane. Figure 5 shows the conversion efficiency of 5-CMC and 8-CMC measured in the temperature range of $150\text{--}250 \text{ }^\circ\text{C}$. As the reaction temperature was increased, the conversion efficiency increased. In particular, the 5-CMC and 8-CMC catalysts exhibit high conversion efficiency values above $200 \text{ }^\circ\text{C}$. Although 5-CMC and 8-CMC exhibited similar trends in conversion efficiency based on the reaction temperature, 5-CMC showed superior catalytic performance for the oxidation of EA compared to 8-CMC. The 5-CMC sample exhibited a high conversion efficiency of 100% during oxidation of EA at $250 \text{ }^\circ\text{C}$. The superior catalytic performance of 5-CMC compared to that of 8-CMC is attributed to the higher specific surface area and pore structure of 5-CMC.

4. Conclusion

A CMC using a simple and efficient co-precipitation method was developed. A high yield and good textural properties of 5-CMC were obtained by controlling the Cu concentration to 0.005 M , reaction time to 30 min, and reaction temperature to $25 \text{ }^\circ\text{C}$. The as-obtained 5-CMC comprised randomly aggregated nanoparticles, resulting in a large surface area of $230.8 \text{ m}^2/\text{g}$ with a mesoporous structure. The catalytic performance of 5-CMC was tested in the oxidation reaction of EA, and the results were compared with those of 8-CMC. Further, 5-CMC exhibited ameliorated catalytic performance than that of 8-CMC in the reaction temperature range of $150\text{--}250 \text{ }^\circ\text{C}$. In particular, 5-CMC had a high conversion efficiency value of 100% for oxidation reaction of EA at a low reaction temperature of $250 \text{ }^\circ\text{C}$. The synthesis method and CMC developed in this study can be used in catalytic thermal oxidizer processes for the oxidation and decomposition of many VOCs at low temperatures.

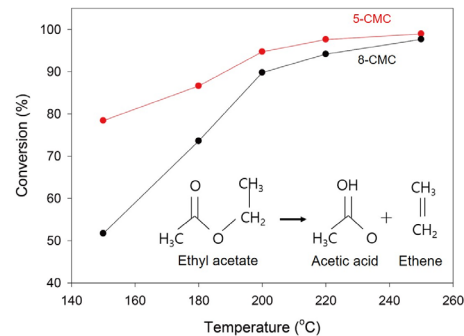


Figure 5. EA conversion efficiency values of 5-CMC and 8-CMC at different reaction temperatures.

Acknowledgement

This work was supported by the Korea Research Institute of Chemical Technology (KRICT) core project (SS2242-10), and supported by a cooperative project as a “Basic project of the Korea Institute of Geoscience and Mineral Resources (KIGAM) funded by the Ministry of Science and ICT of Korea”.

References

1. M. Luo, Y. Cheng, X. Peng, and W. Pan, Copper modified manganese oxide with tunnel structure as efficient catalyst for low-temperature catalytic combustion of toluene, *Chem. Eng. J.*, **369**, 758-765 (2019).
2. B. D. Napruszewska, A. Michalik, A. Walczyk, D. Duraczyńska, R. Dula, W. Rojek, L. Litynska-Dobrzynska, K. Bahrnowski, and E. M. Sewicka, Composites of laponite and Cu-Mn hopcalite-related mixed oxides prepared from inverse microemulsions as catalysts for total oxidation of toluene, *Materials*, **11**, 1365-1379 (2018).
3. T. Biemelt, K. Wegner, J. Teichert, and S. Kaskel, Microemulsion flame pyrolysis for hopcalite nanoparticle synthesis: a new concept for catalyst preparation, *Chem. Commun.*, **15**, 5872-5875 (2015).
4. S. Dey and G. C. Dhal, Synthesis of hopcalite catalyst by various methods for improved catalytic conversion of carbon monoxide, *Mater. Sci. Technol.*, **3**, 377-389 (2020).
5. S. Said, S. Mikhail, and M. Riad, Recent processes for the production of alumina nano-particles, *Mater. Sci. Technol.*, **3**, 344-363 (2020).
6. M. Bannai, A. Houkabe, M. Furukawa, T. Kashiwagi, A. Akisawa, T. Yoshida, and H. Yamada, Development of efficiency-enhanced cogeneration system utilizing high-temperature exhaust-gas from a regenerative thermal oxidizer for waste volatile-organic-compound gases, *Appl. Energy*, **83**, 929-942 (2006).
7. J. R. Hart, Emissions of polychlorinated dibenzo-p-dioxins and dibenzofurans from catalytic and thermal oxidizers burning dilute chlorinated vapors, *Chemosphere*, **54**, 1539-1547 (2004).
8. H. Bai, Z. Wang, J. Zhang, J. Wu, Y. Yue, Q. Liu, and G. Qian, Synthesis of a perovskite-type catalyst from Cr electroplating sludge for effective catalytic oxidation of VOC, *J. Environ. Manage.*, **294**, 113025-113031 (2021).
9. S. Dey and N. S. Mehta, To optimized various parameters of hop-

- calite catalysts in the synthetic processes for low temperature CO oxidation, *Appl. Energy Combust. Sci.*, **6**, 100031-100042 (2021).
10. Y. H. Yap, M. S. W. Lim, Z. Y. Lee, K. C. Lai, M. A. Jamaal, F. H. Wong, H. K. Ng, S. S. Lim, and T. J. Tiong, Effects of sonication on co-precipitation synthesis and activity of copper manganese oxide catalyst to remove methane and Sulphur dioxide gases, *Ultrason. Sonochem.*, **40**, 57-67 (2018).
 11. S. Dey and G. C. Dhal, Deactivation and regeneration of hopcalite catalyst for carbon monoxide oxidation: a review, *Mater. Today Chem.*, **14**, 100180-100191 (2019).
 12. S. Dey and N. S. Mehta, Influence the performances of hopcalite catalysts by the addition of gold nanoparticle for low temperature CO oxidation, *Cleaner Eng. Technol.*, **4**, 100171-100181 (2021).
 13. Y. Xu, Z. Qu, Y. Ren, and C. Dong, Enhancement of toluene oxidation performance over Cu-Mn composite oxides by regulating oxygen vacancy, *Appl. Surf. Sci.*, **560** 149983-149994 (2021).
 14. J. Kim, Y. H. Min, N. Lee, E. Cho, K. Y. Kim, G. Jeong, S. K. Moon, M. Joo, D. B. Kim, J. Kim, S.-Y. Kim, Y. Kim, J. Oh, and S. Sato, In situ spectroscopic and computational studies on a MnO₂-CuO catalyst for use in volatile organic compound decomposition, *ACS Omega*, **2**, 7424-7432 (2017).
 15. H. Lin, D. Chen, H. Liu, X. Zou, and T. Chen, Effect of MnO₂ crystalline structure on the catalytic oxidation of formaldehyde, *Aerosol. Air Qual. Res.*, **17**, 1011-1020 (2017).
 16. M. S. Lee, S.-I. Kim, M. Lee, B. Ye, T. Kim, H.-D. Kim, J. W. Lee, and D. H. Lee, Effect of catalyst crystallinity on V-based selective catalytic reduction with ammonia, *Nanomaterials*, **11**, 1452-1463 (2021).

Authors

Min Jae Kim; Bachelor's Course, Researcher, Department of Chemical Engineering, Kangwon National University, Samcheok 25913, Republic of Korea; kminjae5043@gmail.com

Jo Hee Yoon; M. Sc., Researcher, Department of Chemical Engineering, Kangwon National University, Samcheok 25913, Republic of Korea; sefiraro@gmail.com

Jae-Min Jeong, Ph.D., Senior Researcher, Mineral Resources Research Division, Korea Institute of Geoscience and Mineral Resources, Daejeon 34132, Republic of Korea; jmjeong@kigam.re.kr

Bong Gill Choi; Ph.D., Associate Professor, Department of Chemical Engineering, Kangwon National University, Samcheok 25913, Republic of Korea; bgchoi@kangwon.ac.kr